JMEPEG (2012) 21:424–428
DOI: 10.1007/s11665-011-9935-y

1059-9495/$19.00

Corrosion Resistance of Ti-O Film Modified 316L Stainless Steel Coronary Stents In Vitro

Hengquan Liu, Yongxiang Leng, and Nan Huang

(Submitted October 1, 2010; in revised form March 22, 2011)

This article dealt with improving corrosion resistance of stent modified using Ti-O film. Ti-O films of various thicknesses were grown on the surface of 316L stainless steel (SS) stents by metal vacuum arc source deposition technology, and the phase composition, the thickness and the adhesion between films and substance were investigated by micro-x-ray diffraction (Micro-XRD), surface profilometer, and scanning electron microscopy (SEM) separately. The corrosion resistance of modified stent was assessed by polarization test in phosphate buffered solution (37 ± 1 °C). The result shows that the Ti-O films were very smooth and uniform. There were not any cracks and delaminations after dilation by angioplasty, the adhesion between Ti-O film and stent is satisfactory. The open circuit potential (OCP) of the Ti-O film modified stents was higher than that of the bare stents; it shows that the electrochemical stability of modified stents was more than bare stents. The polarization test result indicates that the passivation stability and anti-breakdown performance of Ti-O film stents had better than bare stents, and no pitting was observed on the surface of both modified stents, but the local film striations were found on the stent surface of the thicker film, which indicated that the Ti-O film stents with certain thickness has good corrosion resistance.

Keywords adhesion, coronary stent, corrosion resistance, Ti-O film

1. Introduction

Generally, stent insertion was a standard procedure to reduce stenosis or blockage of coronary arteries (Ref 1). However, in-stent stenosis has become a new clinical problem for metallic stents because of the corrosive environment in the human body (Ref 2). The released metal ions from the corroded stents not only induce platelet activation which leads to thrombogenicity of the stents but also cause the endothelial cell damage due to the potentially toxic effect of metal ions (Ref 3). The release mechanisms of metal ions include electrochemical corrosion and mechanically accelerated electrochemical processes such as stress corrosion, corrosion fatigue, and fretting corrosion (Ref 4). 316L stainless steel (SS) had been widely used to make coronary stent. Besides Fe, 316L SS contains 13% nickel, 17% chromium, and 2.25% molybdenum. The release of nickel, chromium, and molybdenum ions from 316LSS stent may trigger local immune response and inflammatory reactions, which may in turn induce intimal hyperplasia and in-stent restenosis (Ref 2, 5). The use of a protective film is a viable approach to mitigate excessive corrosion and it also combines the desirable characteristics of different materials (Ref 6, 7). In recent years, synthesizing bioceramic film on stent surface has been attracting considerable attention, since the good mechanical properties of metals and good chemical stability of ceramic films can be combined. Many investigations demonstrated that ceramic films such as DLC, TiN, and SiC, all have good blood compatibility (Ref 8-10). In fact, the wellknown good biocompatibility of titanium is related to the native titanium oxide on its surface (Ref 11, 12), so Ti-O film has potential application on stents to improve the biocompatibility and the corrosion resistance of the stent. The adhesion and uniform of film should be good to ensure a long service life in vivo. Some researchers have reported that it is difficult to deposit a uniform layer of Ti-O film on the stent with complex shapes or geometry by ion beam-assisted deposition or chemical vapor deposition, etc. (Ref 13). Our previous experiments have disclosed that the favorable Ti-O film was obtained by metal vacuum arc source deposition technology, so this technology is a promising method to fabricate Ti-O film on coronary stent.

Various techniques have been developed to evaluate the corrosion resistance of metal materials. Among these, the electrochemical method has frequently been used because it can provide quantitative results via a simple conventional electrochemical apparatus. In this study, the metal vacuum arc sources deposition was used to fabricate various thick Ti-O films on 316L SS stents. The polarization corrosion test in vitro was carried out to study the corrosion resistance.

2. Experimental

2.1 Preparation of Ti-O Film

The 316LSS tube was laser cut, following electrochemical polishing was performed to obtain bare stent. Ti-O films were grown on stent surface using metal vacuum arc sources deposition device. Prior to deposition, the stent surface was

Hengquan Liu and **Yongxiang Leng**, Key Laboratory for Advanced Technologies of Materials, Ministry of Education, Southwest Jiaotong University, Chengdu 610031, China; and **Hengquan Liu** and **Nan Huang,** School of Materials Science and Engineering, Southwest Jiaotong University, Chengdu 610031, China. Contact e-mail: yxleng@263.net.

cleaned by argon ion for 10 min at working pressure 0.6 Pa. And then oxygen was introduced into the vacuum chamber, the partial pressure was 0.2 Pa. The detail technical parameter is shown in Table 1. To obtain different thick films, the 4 and 6 min of deposition time were adopted, respectively.

2.2 Characterization of Ti-O Film

The Micro-XRD spectrum was obtained using a X'Pert Pro MPD (Philips, Netherlands) diffractometer with Cu Kα irradiation (λ = 0.154060 nm) and the morphology of Ti-O film was characterized using the optical microscopy (Motic group-Plus 2.0ML) and SEM (S450, Japan Hitachi). In order to obtain the thickness of various films, a silicon plate was adhered on the side of the frame. The thickness of Ti-O film deposited on silicon plate was measured by surface profilometer (AMBIOS XP-2). The modified stents are mounted on balloon and then deployed under certain pressure; the stents with internal expanded diameters of 3.0 mm were used in this investigation. The adhesion of the film was evaluated via revealing the morphology of Ti-O films by SEM, specifically

Table 1 Technical parameter of Ti-O film

O_2 Flow rate, sccm	Arc source voltage, V	Arc source current, A	Deposited time, min
51	32	0.56	4 or 6

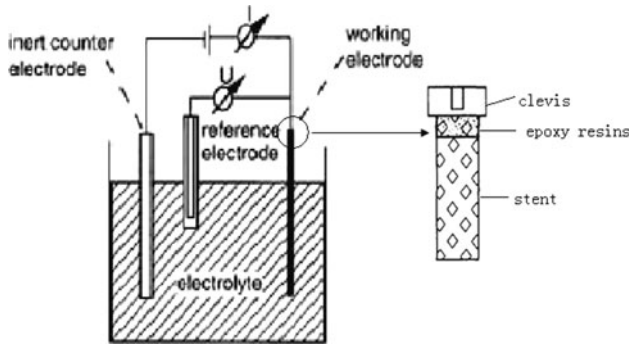

Fig. 1 The diagram of the electrochemical experimental device

maximum deformed cell of the stent undergone compressing or expanding.

2.3 The Measure of Open Circuit Potential (OCP)

The phosphate buffered solution with the normal physiological pH at 7.4 was purged with nitrogen for half an hour prior to immersion. As shown in Fig. 1, the apparatus consisted of a conventional three-electrode cell comprising a working electrode, a saturated calomel electrode (SCE), a platinum sheet as the counter electrode, the clevis used mounting stent was accord to ASTM F 2129. The changes in the OCP were monitored as a function of time under open circuit conditions for approximately 30 min. After 0.5 h immersion in the test solution, a fairly stable potential could be achieved, its value is OCP.

2.4 The Polarization Test

The potentiodynamic polarization measurement was carried out at a scanning rate of 2 mV/s, the polarization scanning was conducted at potentials from −500 to 500 mV (vs.SCE). The electrical charge (Q) was obtained using coulometric method within a certain potential range (Ref 13, 14). As shown in Fig. 2, the time of electron migration would be obtained on this section, coulomb charge could be calculated by integrating current density against this time, and the corrosion rate could be also obtained by Faraday's law (Ref 15):

$$Q = \int_{t_0}^{t_1} I_{(a)}(t)\,\mathrm{d}t \qquad \text{(Eq 1)}$$

$$\begin{aligned}\int_{t_0}^{t_1} f(x)\,\mathrm{d}x &= S_1 + S_3 + \cdots + S_{2n-1} \\ &= \frac{h}{3}(y_1 + 4y_2 + y_3 + y_3 + 4y_4 + y_5 + \cdots \\ &\quad + y_{2n-1} + 4y_{2n} + y_{2n+1}) \\ &= \frac{h}{3}[y_1 - y_M + 4(y_2 + y_4 + \cdots + y_{2n}) \\ &\quad + 2(y_3 + y_5 + \cdots + y_{2n+1})] \\ &= \frac{2(t_1 - t_0)}{3N}\left[\frac{y_1 - y_M}{2} + \sum_{i=1}^{n}(2y_{2i} + y_{2i+1})\right] \qquad \text{(Eq 2)}\end{aligned}$$

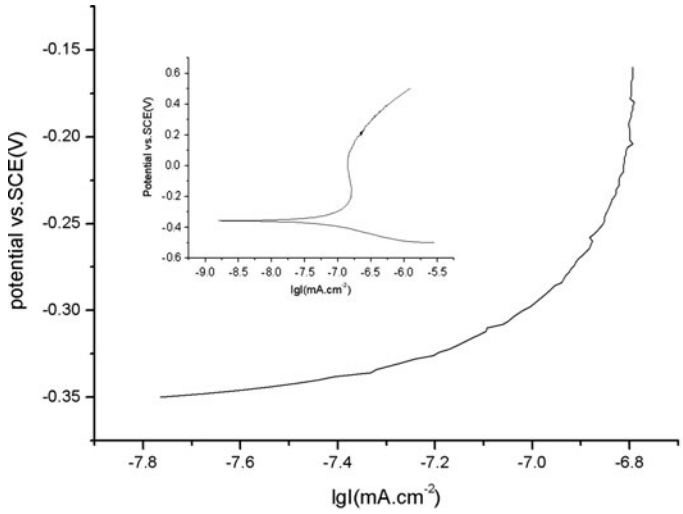

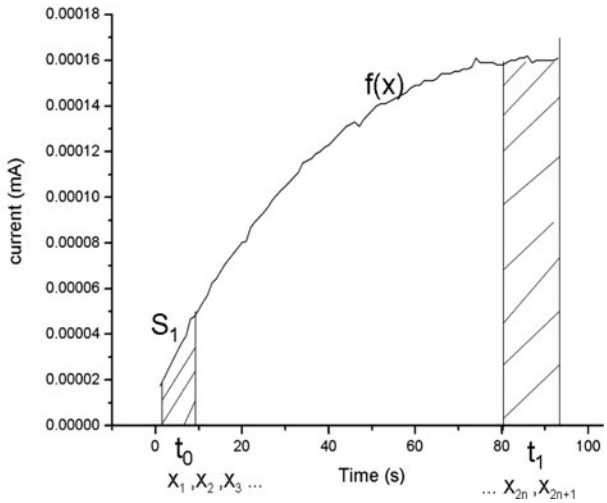

Fig. 2 The delineation of coulomb charge integration

$$m = \frac{MQ}{nF} \quad \text{(Eq 3)}$$

$$v = \frac{m}{\rho_{316L}.S} \times \frac{365 \times 24 \times 3600}{t_1 - t_0} \quad \text{(Eq 4)}$$

where Q, n, m, M, F, S, and v were coulomb charge (mC/cm^2), amount of electron translation, weight loss of stent (mg), atomic weight, Faraday constant, surface area of stent and corrosion rate (mm/a), respectively.

3. Results and Discussion

The microphotograph of the Ti-O film modified stents is shown in Fig. 3. It can be seen that the Ti-O film on the stent surface was favorable smooth and uniform; there is no any crack or particle on stents surface. As shown in Fig. 4, the rutile phase of Ti-O on the modified surface was found from Micro-XRD spectrum.

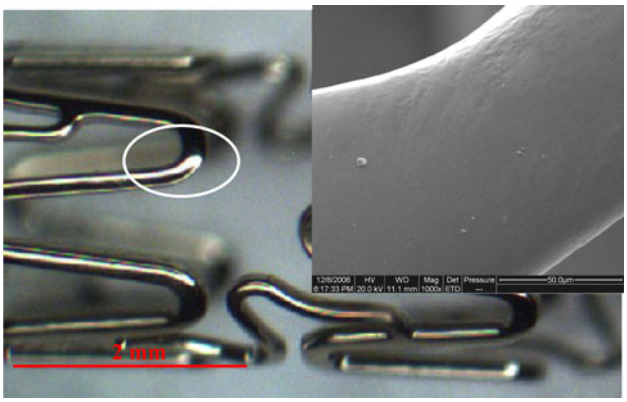

Fig. 3 The morphology images of the Ti-O film modified stent

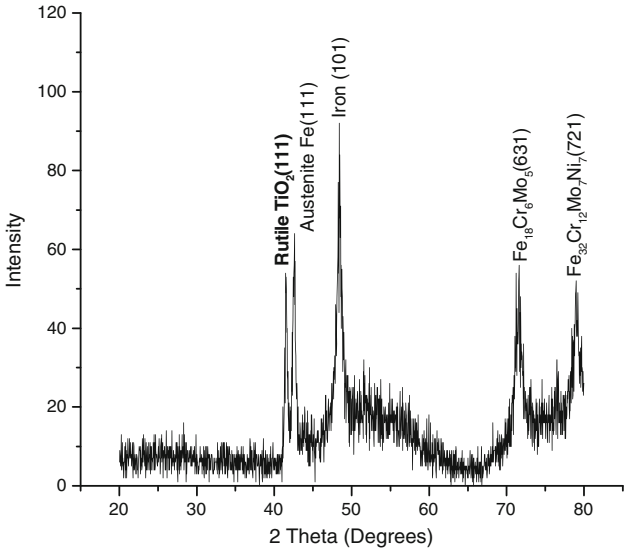

Fig. 4 The Micro-XRD pattern of Ti-O film on stent

The thickness of Ti-O film deposited 4 min is estimated to be 10 nm, which is thinner than that of 21 nm of 6 min. As shown in Fig. 5, the Ti-O film of both modified stents is still smooth and uniform after dilation by angioplasty. There are no any cracks on deformed stent cell, and no delamination and destruction are observed from SEM images, indicating that the Ti-O film can adhere tightly on the stent surface. Furthermore, the Ti-O films of various thicknesses can withstand the compressive and expansion stress imparted during mounting and deployment process.

The evolution with time of the OCP obtained from the bare and modified stents is presented in Fig. 6. Throughout the entire immersion period, the OCP values of the modified stents are much more positive than those of the bare stent. After immersion of approximately 200 s, the OCP value of the bare stent decreases abruptly, and subsequently, the potential fluctuates substantially up to 30 min, indicating that the test solution has reached the substrate and has caused pitting corrosion as well as rapid repair. In contrast, the OCP values measured from the both Ti-O film modified stent do not vary as much. After an initial increase, the OCP value increases slightly with immersion time as a sign of strong surface passivation and electrochemical stability.

Typical polarization curves of bare and Ti-O modified stent are shown in Fig. 7. As shown in Fig. 7, the polarization curves of the modified and bare stents are similar, but the current density of Ti-O modified stent is less than bare stent throughout polarization scanning. The E_{corr} of the Ti-O modified stent is -0.118 versus -0.315 V of bare stents, which indicates more effective inhibition of localized corrosion for modified stents. There is no obvious transitional region from activation to passivation state (Ref 16), and the anti-breakdown property of modified stents is better than bare stent. Nevertheless, dissolution and self-repair owing to defect of films (Fig. 7b) may cause unstable, and these variations may also result in metastable pitting reactions on the stainless steel surface.

In fact, the precise weight loss of the stent owing to the detailed electrochemical corrosion process was associated with the cumulative coulomb charges which were consumed by dissolution in the anodic and passivation region. Therefore, the coulomb charge was another method used to evaluate the corrosion resistance of metal materials. The coulomb charge was obtained by integration of corrosion current against polarization time from the OCP to 120 mV (slightly above which the transpassivation occurs (Ref 13)). The average electrical charges for modified stent were 10.60 mC/cm^2, less than 62.65 mC/cm^2 of the bare stents, evaluating corrosion rate of bare stent was 4.41×10^{-3} mm/a versus 0.75×10^{-3} mm/a of modified stent, indicating the outstanding electrochemical nobility and stability of the Ti-O modified stents.

The SEM micrographs of the all stents after potentiodynamic testing are shown in Fig. 8. Some pits were observed on surface of the bare stent, it suggests the formation of "big cathode/small anode" galvanic couples which were caused by pin-holes or destruction of natural passivating film on the surface of 316L SS. Another reason might be that there was chromium carbides ($Cr_{23}C_6$) precipitated at the grain boundaries, which consumed chromium in boundary region, and resulted in the chromium-depleted areas (Ref 17). Consequently, the potential at the grain boundaries was lower than that at interior grain, so grain boundary as anode of

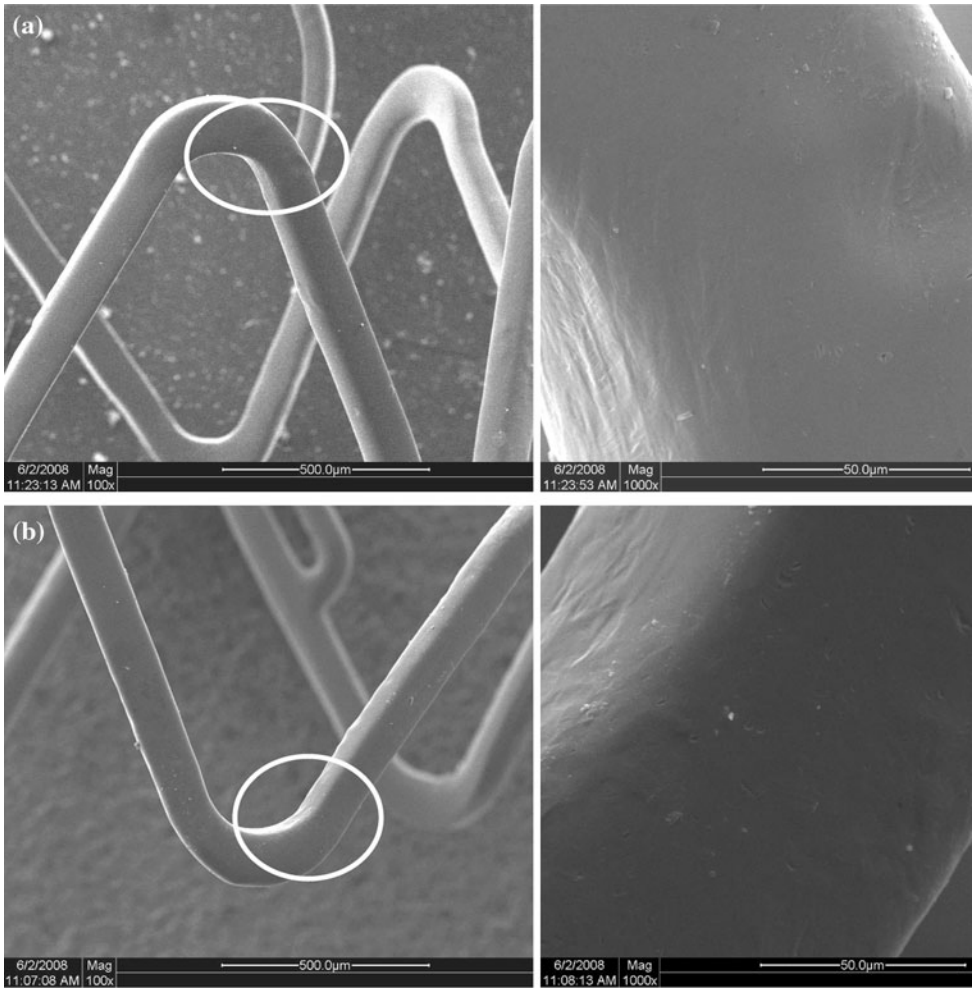

Fig. 5 The morphology photographs of expanded stents: 4 min (a) and 6 min (b) of deposition time separately

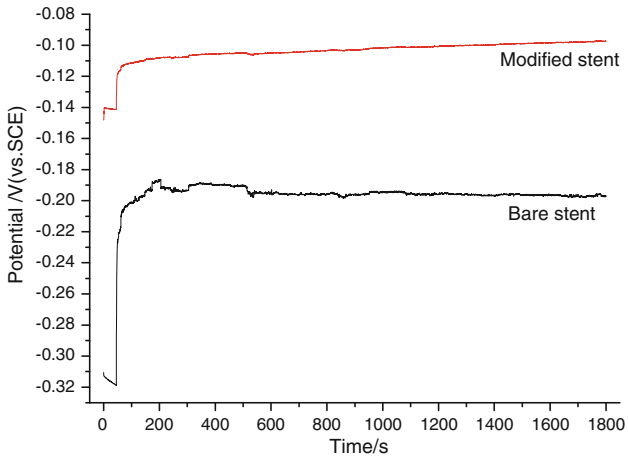

Fig. 6 The evolution of OCP for bare stent and modified stent

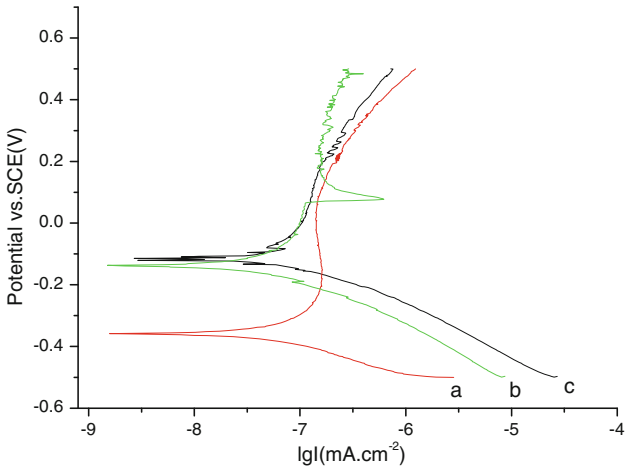

Fig. 7 The polarization curves of the bare (a), modified stents with 4 min (b), and 6 min of deposition time (c)

micro-corrosion cell will be first corroded (Ref 18). Figure 8(b) was SEM micrographs of the Ti-O film modified stent after polarization test. It shows that there was no obvious corrosion for the modified stents, and no pitting was observed on surface of the Ti-O film modified stents. Only some striations were found on the stent surface of thicker film (Fig. 8c), which indicated that the Ti-O film stent with the certain thickness has a good protection for 316L SS stents.

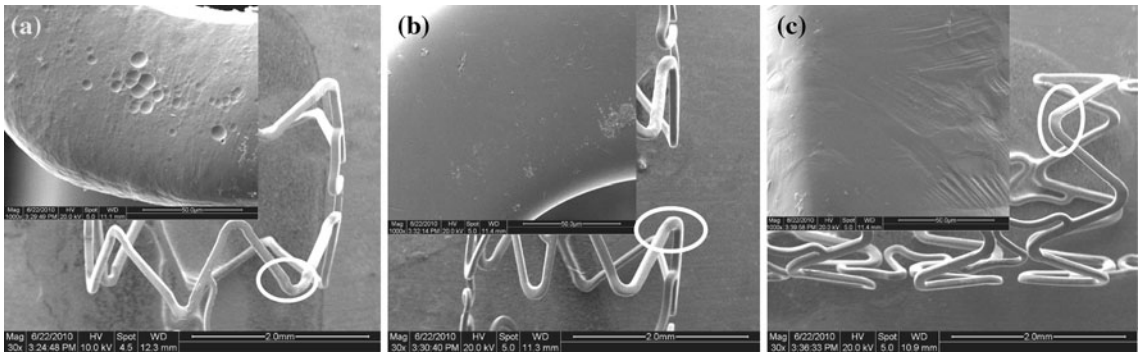

Fig. 8 The SEM micrographs of the stents after polarization test: the bare (a), modified stents with 4 min (b), and 6 min of deposition time (c) separately

4. Conclusions

In same test condition, the OCP of the Ti-O modified stent was higher than the bare stents, and the coulomb charge of the bare stents was almost six times more than that of modified ones. Ti-O film modified stents had better passivation stability and anti-breakdown performance than bare stents. Moreover, the current density of modified stents is less than bare stents throughout polarization scanning. The test results suggested that Ti-O films with certain thickness could prevent 316L SS from corrosion, and may be a potential approach to modify 316L SS coronary stent in clinical work.

Acknowledgments

This study was supported by the Key Basic Research Program 2005CB623904, the Program for New Century Excellent Talents in University (06-0800).

References

1. I.K. Stefanids, V.A. Tolis, D.G. Sionis et al., Development in Intracoronary Stents, *J. Cardiol.*, 2002, **43**(4), p 63–67
2. G. Mani, M.D. Feldam, D. Ptel et al., Coronary Stents: A Materials Perspective, *Biomaterials*, 2007, **28**, p 1689–1710
3. I.B. McPhee and C.E. Swanson, Metal Ion Levels in Patients With Stainless Steel Spinal Instrumentation, *Spine*, 2007, **32**, p 1963–1968
4. N. Hallab, K. Merritt, and J.J. Jacobs, Metal Sensitivity in Patients with Orthopaedic Implants, *J. Bone Joint Surg. Am.*, 2001, **83A**, p 428–436
5. I. Menown, R. Lowe, and I. Penn, Passive Stent Coatings in the Drug-Eluting Era, *J. Invasive Cardiol.*, 2005, **17**, p 222–228
6. F. Airoldi, A. Colombo, D. Tavano et al., Comparison of Diamond-Like Carbon-Coated Stents Versus Uncoated Stainless Steel Stents in Coronary Artery Disease, *Am. J. Cardiol.*, 2004, **93**(4), p 474–477
7. M. Unverdorben, K. Sattler, R. Degenhardt et al., Comparison of a Silicon Carbide-Coated Stent Versus a Noncoated Stent in Human Beings: The Tenax Versus Nir Stent Study's Long-Term Outcome, *J. Interv. Cardiol.*, 2003, **145**(4), p 325–333
8. F. Zhang, Z.H. Zheng, and Y. Chen, In Vivo Investigation of Blood Compatibility of Titanium Oxide Films, *J. Biomed. Mater. Res.*, 1998, **42**, p 128–133
9. T. Yuhta, Y. Kikuta, and Y. Mitamura, Blood Compatibility of Sputter-Deposited Alumina Films, *J. Biomed. Mater. Res.*, 1994, **28**(2), p 217–224
10. M. Amon, A. Bolz, and M. Schaldach, Improvement of Stenting Therapy with a Silicon Carbide Coated Tantalum Stent, *J. Mater. Sci. Mater. Med.*, 1996, **7**, p 273–278
11. L. Tan, C.W. Crone, and K. Sridharan, Fretting Study of Surface Modified Ni-Ti Shape Memory Alloy, *J. Mater. Sci. Mater. Med.*, 2002, **13**(5), p 501–508
12. M.I. Jones, I.R. Mccoll, D.M. Grant et al., Protein Adsorption and Platelet Attachment and Activation, on TiN, TiC, DLC Coatings on Titanium for Cardiovascular Applications, *J. Biomed. Mater. Res.*, 2000, **52**(2), p 413–421
13. C.Z. Cheng, X.H. Shi, P.C. Zhang et al., The Microstructure and Properties of Commercial Pure Iron Modified by Plasma Nitriding, *Solid State Ion.*, 2008, **179**(21–26), p 971–974
14. Y.M. Cheng, G.P. Yu, and J.H. Huang, Comparison of Electrochemical Porosity Test Methods for TiN-Coated Stainless Steel, *Surf. Coat. Technol.*, 2002, **150**(2), p 309–318
15. H.W. Wang and M.M. Stack, Corrosion of PVD TiN Coatings Under Simultaneous Erosion in Sodium Carbonate/Bicarbonate Buffered Slurries, *Surf. Coat. Technol.*, 1998, **105**(1), p 141–146
16. D. Yang and Z. Shen, *Metal Corrosion*, Metallurgy Industry Press, Beijing, 2003, p 58
17. D.A. Jones, *Principles and Prevention of Corrosion*, 1st ed., Macmillan, New York, 1992, p 147
18. Y. Wang and D.O. Northwod, An Investigation of the Electrochemical Properties of PVD TiN-Coated SS410 in Simulated PEM Fuel Cell Environments, *J Hydrogen Energy*, 2007, **32**, p 895–902